Journal of Applied Polymer Science

Comparative Study of the Dielectric Properties of Natural-Fiber–Matrix Composites and E-Glass–Matrix Composites

A. Triki,[1] M. Guicha,[2] Med Ben Hassen,[2] M. Arous[1]

[1]Laboratoire des Matériaux Composites, Céramiques et Polymères, Faculté des Sciences de Sfax, Route de Soukra, 3018, Tunisia
[2]Laboratoire de Recherche Textile, Institut Supérieure des Etudes Technologiques Ksar Hellal, Avenue Hadj Ali Soua, BP 68, Ksar Hellal 5070, Tunisia
Correspondence to: A. Triki (E-mail: trikilamacop@yahoo.fr)

ABSTRACT: In this work, we undertook a comparative study of the dynamic dielectric analysis of two composites: natural-fiber-reinforced unsaturated polyester (NFRUP) and E-glass-mat-reinforced unsaturated polyester (EGMRUP). In both composites, two common relaxation processes were identified, the first of which was the α-mode relaxation associated with the glass transition of the matrix. The second one was associated with conductivity that occurred because of the carriers' charge diffusion and was observed at temperatures above the glass transition and at low frequencies. However, the interfacial or Maxwell–Wagner–Sillars polarization was noticed only in the NFRUP composite. This dielectric study also revealed that compared to E-glass fibers, natural fibers enhanced the thermal insulation in the composite. Also, the study of the fiber adhesion in the matrix with scanning electron microscopy, differential scanning calorimetry, and tensile testing revealed a great compatibility of the fibers with the matrix in both composites. © 2012 Wiley Periodicals, Inc. J. Appl. Polym. Sci. 129: 487–498, 2013

KEYWORDS: composites; microscopy; matrix; reinforcement; relaxation

Received 18 February 2012; accepted 21 August 2012; published online 22 November 2012
DOI: 10.1002/app.38499

INTRODUCTION

Nowadays, natural fibers such as hemp, kenaf, flax, and henequen have gained growing interest, and their study has created fascinating perspectives in several applications. In fact, they have been increasingly used as reinforcements with polymers because they have benefits compared with conventional synthetic reinforcements, such as glass fibers, that power this growing interest.[1,2] These benefits include not only environmental and health concerns but also the sustainability of material resources.

Among the industries that have taken advantage of natural-fiber composites is the automobile industry, which has been leading the way in the use of such composites. Actually, the lower mass density of natural fibers (1.4–1.5 g/cm^3 for flax and hemp fibers vs 2.5 g/cm^3 for glass fibers) leads to a reduction in vehicle weight, which, in turn, leads to a reduction in fuel consumption. The use of natural-fiber composites in automobile interiors also brings about many other benefits, including an increase in safety (the fractures of natural-fiber composites are not as sharp as glass-fiber composites) and improved comfort due to the better acoustic and thermal insulation provided by the natural fibers.[3] Moreover, natural-fiber-reinforced composites are used as substitutes for synthetic-fiber-reinforced composites used in the construction industry because the reinforcement is low in cost and derived from renewable resources.[4]

The most prominent natural fibers used in structural composites are plant fibers because of their specific strength and stiffness compared with that of glass fibers and their accessibility.[5–7] Among these fibers, we can cite alfa, which is the Arabic name of the esparto grass or *Stipa tenacissima* plant. It is widely cultivated in the dry region of North Africa and especially in the center of Tunisia, where it covers about 3500 km^2 with an annual production of 60,000 tons.[8] A great deal of recent research work has been carried out to promote alfa fibers in reinforced polymeric systems,[9–14] which can be applied in automotive industry. Unsaturated polyester (UP) is a popular thermosetting polymer resin used in conventional glass-fiber-reinforced polymer composites. It has been widely used because of its excellent processability and fast crosslinking reaction on the one hand and its good mechanical and chemical properties when fully cured on the other.[15]

Of course, the growth of natural-fiber composites cannot be carried out without any challenge. Indeed, the hydrophilic nature of natural fibers is a potential cause of poor interfacial

adhesion with hydrophobic polymer matrices, and this is considered one of the limitations to some of its exterior uses. The relatively high prices paid for natural-fiber apparel means that the high quality of natural fibers is effectively elevated for composite applications. Almost all natural-fiber products, which currently include nonwoven mats made from low-cost natural fibers at a competitive price to glass fibers, are key to the production of high-performance structured natural composites.[3]

Moreover, natural fibers readily absorb moisture because they contain abundant polar hydroxide groups, which provide the natural-fiber-reinforced polymer matrix composites with a high moisture sorption level.[4] They are also sensitive to environmental conditions in the sense that their physical and mechanical properties depend on the nature of the fiber–matrix adhesion. Indeed, the role of the matrix in a fiber-reinforced composite is to transfer the load to the stiff fibers through shear stresses at the interface. This process requires a good bond between the polymeric matrix and the fibers. Poor adhesion at the interface means that the full capabilities of the composite cannot be exploited. This makes it vulnerable to environmental attacks, which may cause weakness and thus reduce its life span. In other words, insufficient adhesion between the hydrophobic polymers and hydrophilic fibers results in poor mechanical properties in natural-fiber-reinforced polymer composites.

The aforementioned properties may be improved by physical treatments (e.g., cold plasma treatment, corona treatment) and chemical treatments (e.g., maleic anhydride, organosilanes, isocyanates, sodium hydroxide, permanganate, and peroxide treatments).[16,17] Indeed, it has been shown that the pretreatment of the natural fibers with chemical methods (e.g., the use of coupling agents, e.g., silane compounds) enhances the adhesion at the fiber–matrix interface and reduces the moisture sorption of these fibers. As a result, the retention of natural-fiber-reinforced polymer matrix composites under environmental aging in the mechanical properties is improved. In addition, the amount of moisture sorption can be reduced significantly through the replacement of natural fibers with a small amount of synthetic fibers, such as glass or carbon.[18] Many techniques have been used to provide evidence for the effect of these treatments on the fiber–matrix interfacial adhesion. The ones mostly used are dynamic mechanical analysis and scanning electron microscopy (SEM) observation. However, alternative methods that are able to discover the interface and help to better adapt the appropriate coupling agent according to the fiber's surface and the matrix are still attracting much attention. Accordingly, many experimental studies have pointed out the significance of dielectric spectrometry as an additional technique that can be used to probe the composite interface and investigate the effect of fiber treatment on the evolution of composites' interfacial properties.[12,13,19,20]

In this study, nonwoven alfa, wool, and thermobinder fibers [poly(ester terephthalate) (PET)–polyethylene (PE)]-reinforced UP resin composite [natural-fiber-reinforced unsaturated polyester (NFRUP)] were prepared, and their dielectric properties were compared with conventionally reinforced E-glass-mat-reinforced unsaturated polyester (EGMRUP). Two common relaxation processes in both composites were identified and attributed to the glass transition of the matrix and the conductivity, respectively. A third dielectric relaxation was identified only in the NFRUP composite and was attributed to the interfacial or Maxwell–Wagner–Sillars (MWS) polarization, which was accredited to the accumulation of charges at the fiber–polyester resin matrix interfaces. This interfacial relaxation was absent in the EGMRUP composite. In addition, this comparative study confirmed that in contrast to E-glass, the natural fibers enhanced the thermal insulation in the composites. To study the fiber adhesion in the matrix for both composites, a dielectric study was accomplished by SEM, differential scanning calorimetry (DSC), and tensile testing analysis. All of these analyses revealed similar fiber–matrix adhesion characteristics in both composites, and this led to the conclusion that for stiffness applications, NFRUP composites could compete with EGMRUP composites as surface coatings for the inner part of buses.

EXPERIMENTAL

Materials

The UP matrix used in this research work was the same as that used in our previous study[20] and was supplied by Cray Valley/Total (Sousse in Tunisia). In fact, the matrix was mixed with the initiators methyl ethyl ketone peroxide and cobalt octanone at a concentration of 1.5% w/w before the alfa fibers were introduced. The alfa fibers extracted from the plant were attacked chemically by an NaOH solution and were bleached in an NaClO solution. Then, they were separated mechanically with a Shirley analyzer (Ksar Hellal in Tunisia). Because the elaboration of nonwoven fibers with only alfa fibers were not possible because of the noncohesion between them, the latter were mixed with wool fibers to ensure cohesion. Natural fibers on their own cannot be thermoformed and require the addition of polymeric fibers to act as binders, so the added thermobinder fibers were composed of PET and PE as a cover. The obtained sheet of nonwoven fibers was made up of these three kinds of fibers. The diameters of the alfa and wool fibers were 204.86 and 37.21 μm, respectively. The length of the thermobinder fibers was 51 mm; its count was 4 deniers, and their melting temperatures were 260 and 110°C, respectively. The relative volume fractions of these fibers in the composite NFRUP had a ratio of alfa to wool to PET–PE of 17:1:2. To prepare the sheet of nonwoven fibers (alfa + wool + PET–PE), four steps were followed. First, the alfa, wool, and polymeric fibers (PET–PE) were separately cleaned and opened with an industrial bale opener (two passes). Afterward, to improve blending, two other passages through the bale opener were necessary. Next, the fibers were combed into a web by a carding machine, which was a rotating drum or series of drums covered in fine wires. Finally, because the obtained web, whose fibers were unbonded in form, had little strength, it had to be consolidated in some way. In our case, two types of consolidation were used, the first of which was a mechanical bonding with a needle punch. Hence, the web was strengthened by interfiber friction as a result of the physical entanglement of the fibers by needles. We used a laboratory needle-punching machine (two passes were needed). The second consolidation of the nonwoven fiber sheet was a thermal one. Indeed, the presence of the thermobinder fibers in the

sheet allowed the adhesion between fibers, which were under adapted temperature conditions. For this reason, the sheet was deposited in an air oven at a temperature of 120°C, and the sheet was passed through. The PET–PE fibers were submitted to an increase in temperature. The binding was accomplished by a combination of heating, flowing, and cooling. Indeed, the initial calorific energy weakened the outer surface of the thermobinder fibers (PE fibers with a low melting temperature of 110°C), which increased the contact surface with the other fibers, and then, the supplementary energy turned the outer binder into a fluid, which, in turn, molded the natural fibers with the thermobinder ones. After this consolidation, the nonwoven fibers were calendered at 120°C in an industry of developing nonwoven materials to decrease the thickness of the sheet. The E-glass fibers are supplied from a Tunisian company named (STIA: Société Tunisienne de l'Industrie Automobile, Sousse in Tunisia). They were presented in a sheet in which the fibers, whose average length was about 50 mm, were randomly oriented.

Composite Processing

The composites (NFRUP, EGMRUP) were manufactured with the classical contact mold method.[21] In fact, the fibers were deposited on the mold and impregnated with the liquid resin mixed with suitable proportions of methyl ethyl ketone peroxide and cobalt octanone as hardener and catalyst, respectively. The saturated materials were then pressed by a roller to remove bubbles. After the hardness of the resin was measured, the composites were withdrawn from the mold. The obtained NFRUP and EGMRUP composites had 5.2 and 5.5% fiber volume fractions, respectively.

Measurements

SEM. The morphologies of the composite surfaces were observed at room temperature by a Philips XL30 SEM instrument. A gold coating of a few nanometers in thickness was formed on the surfaces of the samples to prevent charging, and the surfaces were examined at an accelerating voltage of 20 kV. These observations were conducted on the upper surface and the cross-sectional surface of the composite so that the longitudinal and cross-sectional aspects of the fibers, respectively, could be observed. For this reason, the sample was cut with a saw at room temperature in the direction of the composite cross-sectional surface and perpendicular to the fiber axis.

DSC. DSC was used to evaluate the glass-transition temperature (T_g) of the matrix and its NFRUP and EGMRUP composites. Samples weighing between 10 and 15 mg were placed in a hermetic pan and sealed. A Jade DSC instrument (PerkinElmer) was operated in the temperature interval −50 to 150°C in a nitrogen environment purged at 20 mW and according to a heating–cooling–heating cycle. In the first heating step, the samples were heated from −50 to 150°C at a heating rate of 5°C/min. Then they were cooled from 150 to −50°C at a cooling rate of 5°C/min. In the second heating step, the samples were heated from −50 to 150°C at a heating rate of 5°C/min. The thermograms were analyzed to estimate the T_g values of the resin and its composites. The T_g value of each sample was determined from the midpoint value of the jump in heat flow in the second heating run. The construction of the lines was done by Pyris software, Perkin Elmer from Courtaboeuf, France.

Tensile Testing. Tensile testing of the NFRUP and EGMRUP composites was carried out with a Lloyds Dynamometer universal testing machine as per NF T 57-301 at a crosshead speed of 5 mm/min and a gripping length of 100 mm (Ksar Hellal in Tunisia).[22] The specimen was cut out in the direction of nonwoven production. All of the results were calculated as the average of 10 samples for each test.

Dielectric Analysis. Dielectric measurements were conducted with an Alpha dielectric–impedance analyzer (Novocontrol, Sfax in Tunisia), with the measurements of the studied samples taken over the temperature range from the ambient to 150°C and in a frequency interval from 10^{-1} to 10^{6} Hz. A circular gold electrode (2 cm in diameter) was sputtered on both surfaces of the sample to ensure good electrical contact with the gold-plated measuring electrodes. A sinusoidal voltage was applied to create an alternating electric field that produced polarization in the sample, which oscillated at the same frequency as the electric field but had a phase angle shift (δ). This phase angle shift was measured by the comparison of the applied voltage with the measured current, which was divided into capacitive and conductive components. With the following equations,[23] the dielectric parameters were calculated:

$$\varepsilon* = \varepsilon' - j\varepsilon'' \tag{1}$$

$$\varepsilon' = \frac{C_{p(\text{sample})}\, d}{\varepsilon_0 A} \tag{2}$$

$$\varepsilon'' = \frac{G_{(\text{sample})}\, d}{\omega \varepsilon_0 A} \tag{3}$$

where $(j)^2 = -1$; ε' and ε'' are the real and imaginary parts of the complex permittivity (ε^*); tan δ ($=\varepsilon''/\varepsilon'$) is the dissipation factor; A and d are the area and thickness, respectively, of the sample; C_p is the capacitance; G is the conductance; and ε_0 is the permittivity of the free space and is equal to 8.854×10^{-12} F/m.

Two kinds of dielectric experiments were carried out. One of them was an isochronal run with fixed frequencies and various temperatures from ambient to 150°C with a heating rate of 2°C/min in a nitrogen atmosphere. The second was an isothermal run with fixed temperatures and scanning frequencies from 10^{-1} to 10^{6} Hz.

RESULTS AND DISCUSSION

SEM Observation

SEM observation was made to explore the fiber–matrix interface in the NFRUP and EGMRUP composites. The SEM micrographs of the composites are displayed in Figures 1(a-d) and 2(a-d). Figure 1(a,b) shows the micrographs of the longitudinal fiber aspects for the NFRUP composite. These micrographs illustrate that the fibers were randomly dispersed in the matrix and that the individual separation of the fibers were not in the form of single fibers. Figure 1(c,d) shows the micrographs of the longitudinal fiber aspects for the EGMRUP composite. This figure shows that the glass fibers were identical and were in the form of single fibers because they were synthetic. The analysis of Figure 1(b,d) illustrated some physical contacts between the fibers and the matrix. Figure 2(a–d) depicts the micrographs of

Applied Polymer SCIENCE

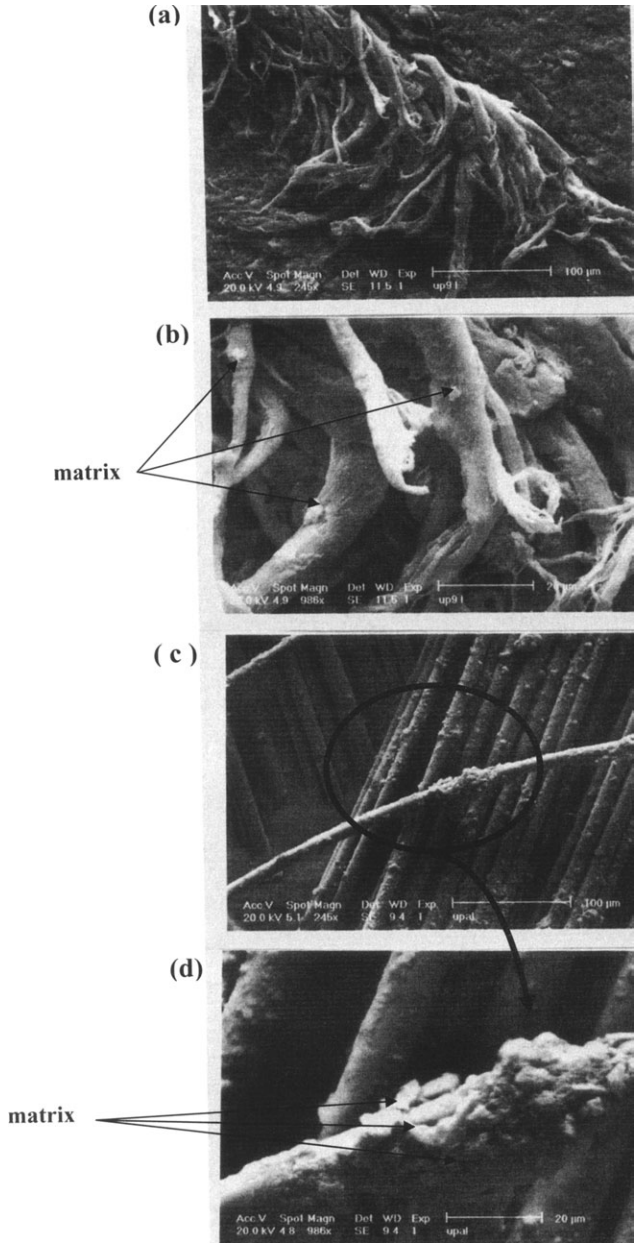

Figure 1. SEM micrographs of the longitudinal fibers aspects for the composites: (a) 100 μm of NFRUP, (b) 20 μm of NFRUP, (c) 100 μm of EGMRUP, and (d) 20 μm of EGMRUP.

the polished cross sections of the NFRUP and EGMRUP composites. Figure 2(a) shows the cross section of a natural fiber, and Figure 2(c) shows the double aspects of the glass fibers, which were randomly dispersed in the matrix, that is, longitudinal fibers aspects and fibers cross-sectional aspects. In Figure 2(b), a closer observation of the interface in the micrographs of the NFRUP composite proved better close contact between the fibers and the matrix than that in the case of the UP film filled with palm tree fibers studied by Kadami et al.[24] In addition, Figure 2(b) reveals a tiny and narrow gap around the fiber that may have eventually led to cracking in the NFRUP composite because fatigue crack propagation resistance depends on the matrix–fiber adhesion.[25–27] However, Azimi et al.[25] reported

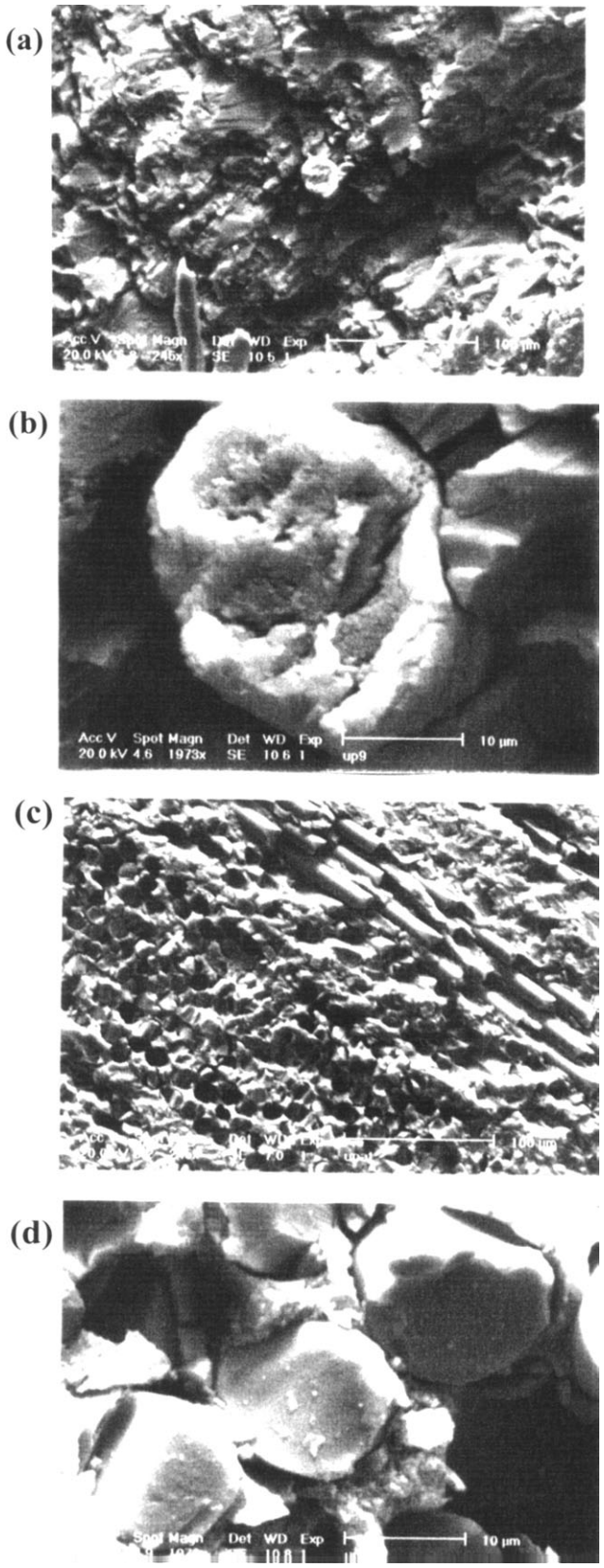

Figure 2. SEM micrographs of the polished cross sections for the composites: (a) 100 μm of NFRUP, (b) 10 μm of NFRUP, (c) 100 μm of EGMRUP, and (d) 10 μm of EGMRUP.

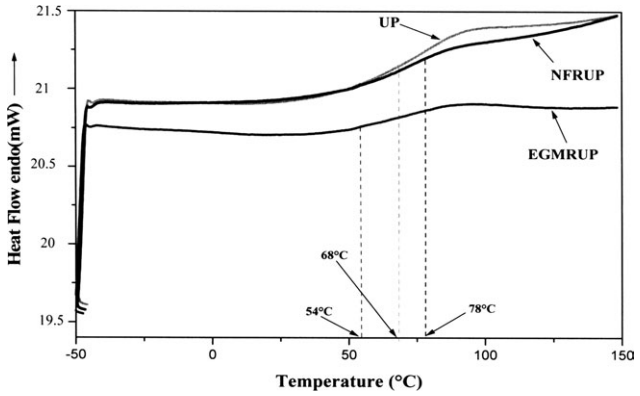

Figure 3. DSC thermograms of the matrix and its composites (NFRUP and EGMRUP) in the second heating run.

that hybrid composites showed significant improvement in fatigue crack propagation resistance, and this could support the NFRUP hybrid composite, which contained two natural fibers (alfa and wool) and the polymeric fibers (PET–PE). A closer look at the E-glass-fiber cross-sectional aspects depicted in Figure 2(d) demonstrated a similar close contact in the interfacial region between the fibers and the matrix compared with that of the NFRUP composite.

DSC

The UP resin matrix and its NFRUP and EGMRUP composites were subjected to DSC to evaluate their thermal properties. The thermographs of all of the samples are shown in Figure 3. The T_g value of each sample was determined from the midpoint value of the jump in heat flow after the second heating run. Also, the line construction was done by the Pyris software, and the obtained values were about 68, 78, and 54°C for the resin and the NFRUP and the EGMRUP composites, respectively. These results indicate that T_g, which was attributed to the transition from a glasslike form to a rubbery and flexible form, increased with the addition of the natural fibers to the matrix. However, this temperature decreased with the addition of E-glass fibers to the matrix. Changes in the glass-transition temperature (ΔT_g) can indicate altered polymer chain mobility. Indeed, depending on the strength of the interaction between the polymer and the filler, this region can have a higher or lower mobility than the bulk material, and this can result in a decrease[28] or an increase[29] in T_g.[30] So ΔT_g is less than 0 if there is a depletion of segments at the boundaries, and ΔT_g is greater than 0 if the segment–filler interactions are strong in comparison with the segment–segment interactions.[31–34] Furthermore, it was argued by extension[35] that if the system is asymmetric (bounded by a free surface and a substrate), ΔT_g is greater than 0 if the monomer–filler interactions are sufficiently strong to dominate the depletion of chain segments near the free surface; otherwise, ΔT_g is less than 0. Moreover, a comparative study carried out of the thermal properties between a functionalized carbon nanotube (CNT)–epoxy composite and a nonfunctionalized CNT–epoxy one revealed a stronger shift in T_g in the case of the composite containing functionalized CNTs. According to this study, it was assumed that covalent bonds between the amino functions on the surface of the CNT and the epoxy would lead to an even stronger reduction in the matrix mobility, which is expressed by a stronger shift in T_g.[36] The different behaviors of the two sample series provided further evidence of the influence of the chemical functionalization of the surface on the interfacial adhesion between the nanotubes and the epoxy resin.

Tensile Properties

The interface adhesion between the reinforcing fiber and the matrix markedly influenced the mechanical performance of the composites.[37,38] This region is the site synergy in composite materials, as the stress redistribution from the matrix to the fibers takes place through their bond/interphase.[39] Therefore, although the interface region appeared to have an insignificant volume fraction, its influence on the overall material properties was significant.[40,41] Indeed, it has been observed that the existence of this interface/interphase brings about significant changes in the relaxation behavior of T_g, as discussed earlier.[42,43] Figure 4 illustrates the traction curves of the NFRUP and EGMRUP composites. Both curves showed a plateau at the beginning for a low strength attributed to the slide of the specimen in the grips of the dynamometer. After this plateau, the curves exhibited a typical mechanical behavior in each composite. On the NFRUP composite traction curve, a depression was observed, which could be explained by the stretching of some fibers. Indeed, the tensile properties of the alfa fibers were lower than those of the E-glass fibers,[44] and this explained the absence of such a depression on the EGMRUP composite traction curve. Accordingly, Figure 5(a–c) shows the Young's modulus, strength, and stress at break of the NFRUP and EGMRUP composites. From these histograms, we observed that the tensile properties of the NFRUP composite were slightly better than those of EGMRUP with regard to the obtained values of the Young's modulus and tensile strength at break values. This showed, according to the Young's modulus, a good cohesion of the materials to transfer stress from the matrix to the fiber.[45] However, the stress at break of the EGMRUP composite was superior to that of the NFRUP composite; this could be attributed to the greater strength of the E-glass fibers compared to that of the natural fibers, as mentioned previously. When specific properties were compared, the differences in the tensile performance became more marked. In fact, the NFRUP composite exhibited

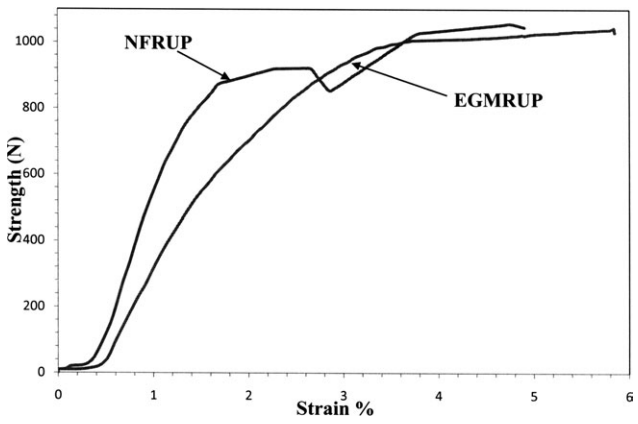

Figure 4. Traction curves of the composites NFRUP and EGMRUP.

Applied Polymer SCIENCE

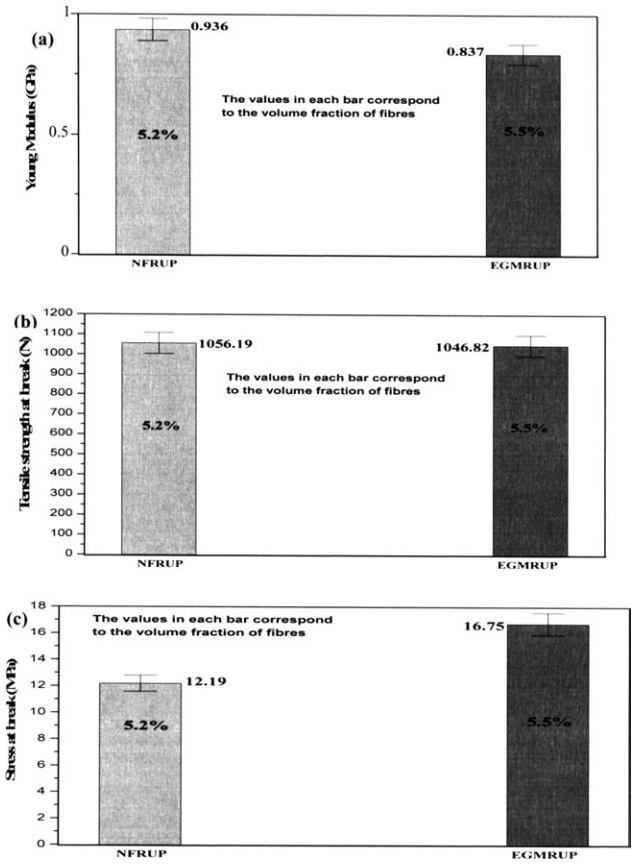

Figure 5. (a) Young's modulus, (b) tensile strength at break, and (c) stress at break of the NFRUP and EGMRUP composites.

superior specific tensile properties than the EGMRUP composite, as shown in Table I. Similar results were found by Arbelaiz et al.[45] in treated flax fiber–polypropylene (PP) composites. Many experimental investigations have been done from this perspective to compare the mechanical properties of natural-fiber–matrix composites with E-glass–matrix composites.[46,47] Indeed, Oksman[48] found that the stiffness of natural-fiber-mat-reinforced thermoplastics with higher or at least the same fiber content was comparable with that of glass-fiber composites. Therefore, for rigidity applications, flax fiber bundle–PP composites could compete with glass–PP composites.[47] On the other hand, it is known that natural-fiber-reinforced polymer matrix composites show lower modulus and strength values and poorer moisture resistance than glass-fiber-reinforced composites.[49] One possibility for obtaining a composite with better mechanical performance is the reinforcement by two or more types in a single matrix; this led to a great diversity of material properties.[50] The advantage of using a hybrid composite is that one type of fiber can complement what is lacking in the other. In our case, the NFRUP composite was a hybrid composite with two natural fibers (alfa and wool) and polymeric fibers (PET–PE), which acted as thermobinder fibers, so the hybridization of the NFRUP composite explained the enhancement of their tensile properties compared to those of the EGMRUP composite. In addition, the alfa fibers were soaked for chemical extraction and bleached in an NaClO solution, and this could have contributed to the improvement of the interaction between the fibers and the matrix. Indeed, it was observed that the interfacial shear strength of hemp-fiber-reinforced UP composite increased when the hemp fibers were treated with sodium hydroxide.[38] This was explained by the greater esterification between alkali-treated hemp fibers with UP. It appeared that the removal of pectin and waxy materials from the surface of untreated hemp fibers, for alkali-treated fibers, increased the number of available OH groups for greater esterification with the UP matrix. Also, Kumar et al.[51] developed a study on the compatibility of unbleached and bleached bamboo fibers with a linear low-density polyethylene matrix, in which they showed that the bleached fibers had more compatibility with the matrix. They demonstrated that during bleaching, some materials (lignin moieties, natural waxes, and pectins found in cellulose fibers, etc.) of high water adsorption capacity might have been dissolved from the delignified fiber; hence, the bleached bamboo fibers could take up less water. They found that the thermal and mechanical properties of the bleached bamboo fibers were also better than those of the unbleached bamboo fiber composites; this further supported the benefit of using bleached bamboo fibers as reinforcement materials.

Dielectric Properties

Comparative plots of the frequency dependence of the dielectric permittivity (ε') and the dissipation factor (tan δ) in the UP resin matrix and its NFRUP and EGMRUP composites for different temperatures from 40 to 150°C in increments of 10°C are shown in Figures 6(a–f). An overall increase in ε' with temperature at low frequencies and a decrease of the behavior with increasing frequency were observed. Also, the dielectric loss factor (tan δ) displayed the presence of two relaxations, which depended on the temperature and frequency, for the matrix and its NFRUP composite and only one relaxation for the EGMRUP composite. Indeed, for the resin, these relaxations were related to an electrode polarization for low frequencies and to the glass transition for the high frequencies when the temperature increased. The latter was associated with the glass–rubbery transition of the polymer. Its relaxation peak maximum shifted to higher frequencies with increasing temperature because the increased temperature resulted in faster movement, which led to

Table I. Tensile Properties of the NFRUP and EGMRUP Composites

Composite material	σ_t (MPa)	σ_t/ρ (MPa cm^3/g)	E_t (GPa)	E_t/ρ (GPa cm^3/g)
NFRUP	12.19± 0.61	12.0 ± 0.6	0.936 ± 0.046	0.92 ± 0.05
EGMRUP	16.75 ± 0.83	7.40 ± 0.37	0.837 ± 0.041	0.37 ± 0.02

σ_t, ρ and E_t are the stress at break, the density and the Young's modulus of the composites respectively.

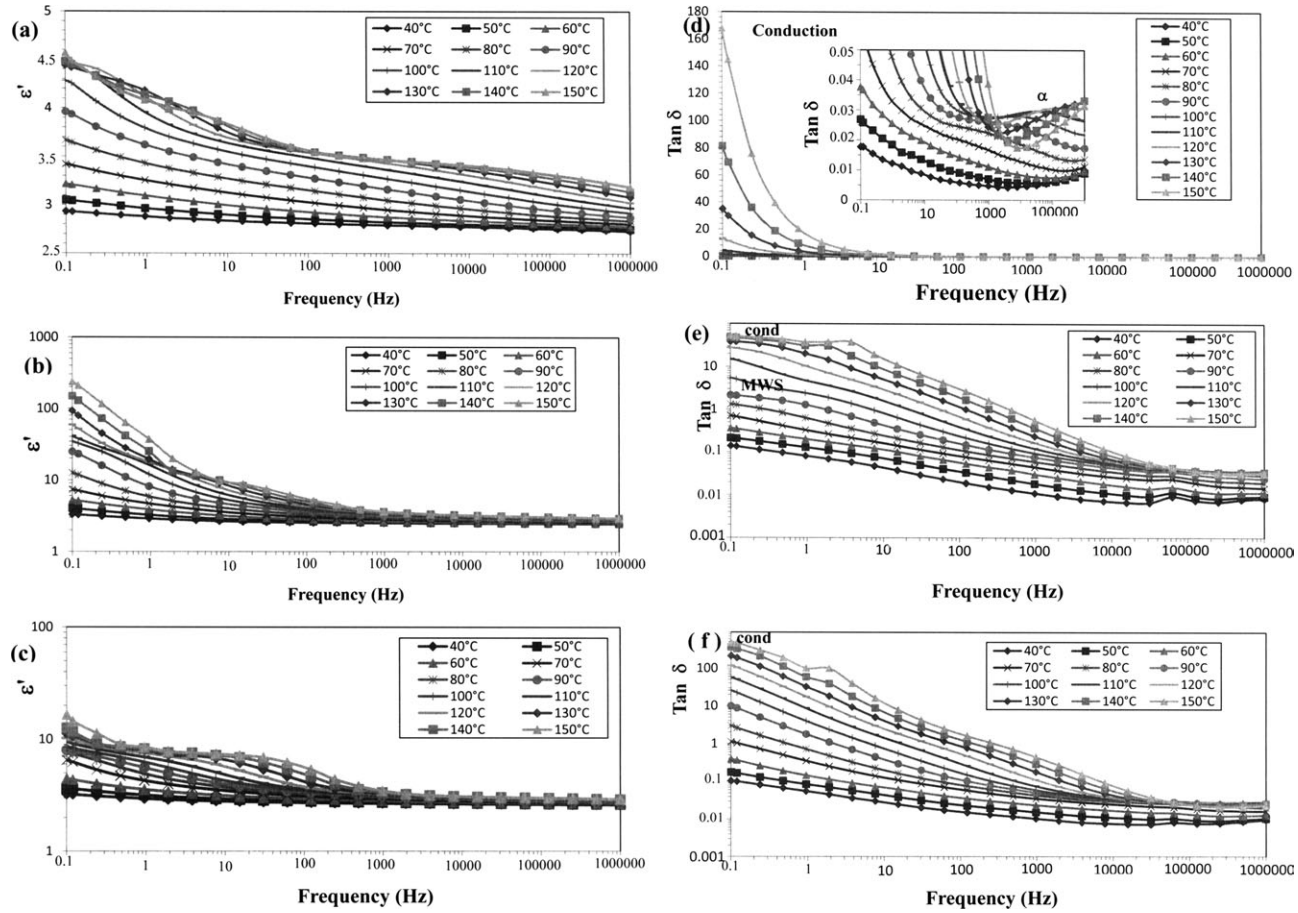

Figure 6. Isothermal runs of the dielectric permittivity (η') and of the dissipation factor (tan δ) versus frequency for the (a,d) polyester matrix and its composites (b,e) NFRUP and (c,f) EGMRUP, respectively.

decreased relaxation times (τs) and shifted the maximum to higher frequencies.[52]

In the case of the NFRUP composite, in addition to the relaxation associated with the direct-current (dc) conductivity effect above T_g, the dissipation factor curves revealed the presence of a relaxation attributed to the MWS effect.[53] This relaxation was the result of the charge accumulations between the fibers and matrix having different conductivities and permittivities.[54] Therefore, the enhancement of these relaxations above T_g amplified the ε' intensity as the temperature increased. It was noted that the interfacial polarization was not visible in the case of the EGMRUP composite. It is also worthwhile to note that previous experimental work on molecular relaxation in an anistropic composite based on hydroxypropyl cellulose and acrylic polymer showed that at low frequencies,[55] the ionic conductivity dominated the dielectric spectra of the composite. Furthermore, Perrier[56] revealed in a study on MWS relaxations in polystyrene–A-glass bead composites that the MWS relaxation process in composites consisting of an insulating matrix loaded with fillers made of a more conductive material depended on the volume fraction of the filler and their size. In our case, the E-glass fibers were less conductive than A-glass fibers.[57] This proved the electrical characteristics of the constitutive elements of the composite (the permittivity and conductivity of the matrix and fillers) to be less different for the appearance of MWS polarization,[56] so the absence of the MWS peak in the tan δ curves, as illustrated in Figure 6(f), which resulted in the slow enhancement of the permittivity ε' at low frequencies and high temperatures in comparison to that of the NFRUP composite, could be explained.

The incorporation of natural fibers into the matrix also led to a decrease in the intensity of the dissipation factor, and this was amplified in reverse in the E-glass fibers. We recognize that the measurement of the dissipation factor of insulating material is important because the loss tangent is a measure of the alternating-current electrical energy, which is converted to heat in an insulator. Such heat raises the insulator temperature and accelerates its deterioration, so natural fibers enhance the thermal insulation in composites.

The α relaxation, which was already seen in the polyester resin, was completely masked by the dc conductivity effect in the case of the EGMRUP composite and by interfacial polarization in the case of the NFRUP composite. Indeed, the maximum of tan δ for the α relaxation of the matrix was 2.58×10^{-3} for a temperature of 90°C and a frequency of 3.91×10^{3} Hz. Nevertheless, in the case of the NFRUP and EGMRUP composites, the isothermal runs of the dissipation factor (tan δ) in the same temperature range showed an enhancement in the intensity and

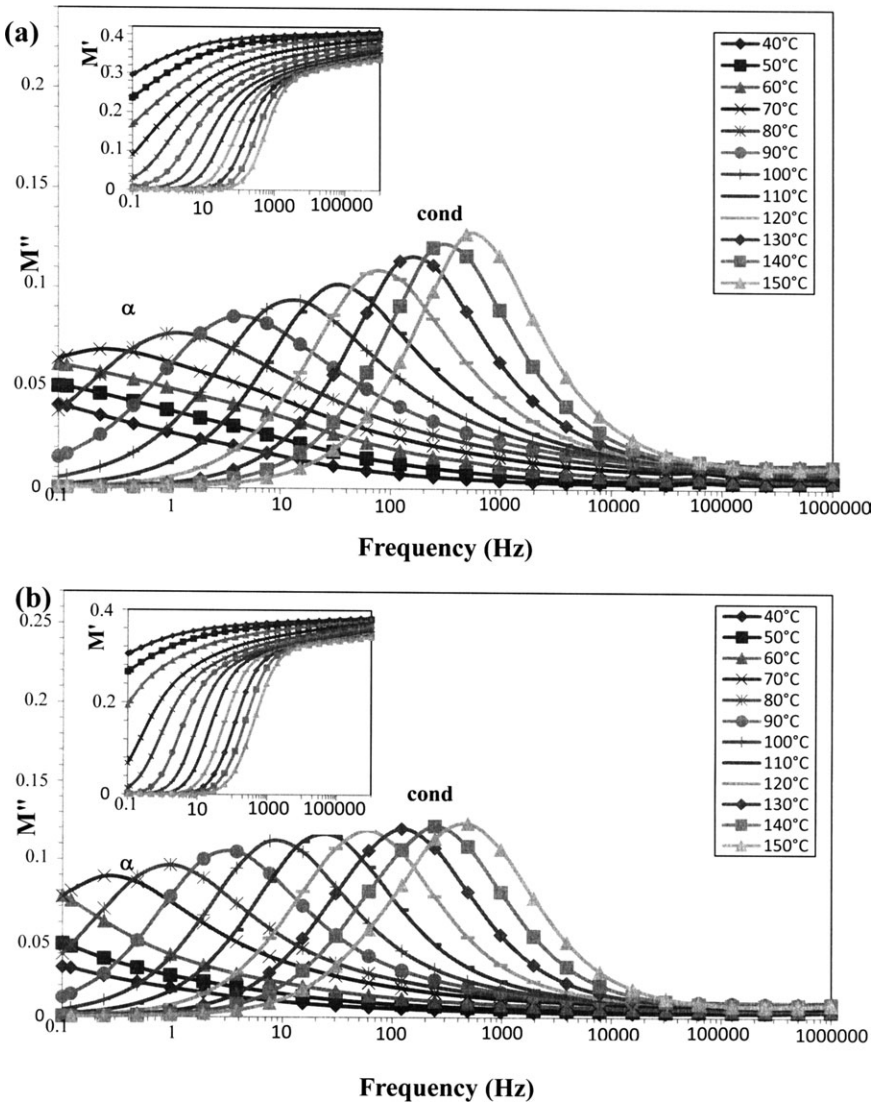

Figure 7. Frequency dependence of M' and M'' for the (a) NFRUP and (b) EGMRUP composites.

appearance of a relaxation peak associated with the interfacial polarization for the NFRUP composite. The same result was observed by Okrassa et al.,[55] in which the α relaxation of the hyroxypropyl cellulose related to its glass transition was not visible in the dielectric spectra. This behavior was connected with the presence of strong hydrogen bonds between cellulose chains.

As already shown, the dc conductivity can hide the α relaxation in dielectric spectra, so to minimize this effect, the formalism of the electric modulus (M^*) or inverse ε^* was introduced. This M^* has recently been adapted for the investigation of dielectric processes occurring in composite polymeric systems and those proposed for the description of systems with ionic conductivity.[12] M^* is defined by Eq. (4):[58]

$$M* = \frac{1}{\varepsilon*} = \frac{1}{\varepsilon' - j\varepsilon''} = \frac{\varepsilon'}{\varepsilon'^2 + \varepsilon''^2} + j\frac{\varepsilon''}{\varepsilon'^2 + \varepsilon''^2} + M' + jM'' \quad (4)$$

where M' and M'' are the real and imaginary parts of the electric modulus, respectively. An advantage of using M^* to interpret bulk relaxation properties is that the variation in the large values of the real part of the permittivity and the loss factor at low frequencies are minimized. In this way, common difficulties of the electrode nature and contact, space-charge-injection phenomena, and absorbed impurity conduction effects, which appear to hide the relaxation in the permittivity representation, can be solved or even ignored.[59]

With this M^* formalism adopted, Figure 7(a,b) shows the similar behavior of M'' as a function of frequency for the NFRUP and EGMRUP composites when they were heated over the temperature range from 40 to 150°C. The inset of each figure exhibits the isothermal variation of the M' frequency dependence. The value of M' was nearly zero at low frequencies and high temperatures; this indicated that the electrode polarization gave a negligibly low contribution to M' and could be ignored.[60,61] After this initial low value, M' increased steeply in the range of 10. A series of two distinct relaxations could be considered for each composite. The first one was related to the α relaxation associated with the glass–rubbery transition of the

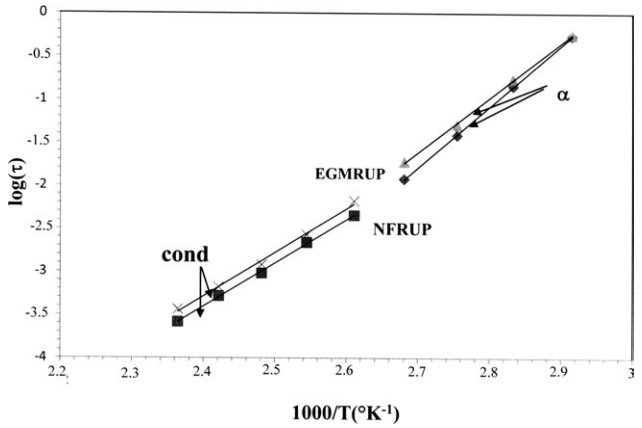

Figure 8. Arrhenius plots of the τ values versus the reciprocal temperature for the NFRUP and EGMRUP composites.

polymer, and the second one, which appeared at high temperatures, was attributed to an ionic conduction effect. To further support these assignments, the activation energy (E_a) relative to the different relaxations was evaluated with the following Arrhenius relation:

$$\tau = \tau_0 \exp\left(\frac{E_a}{k_B T}\right) \tag{5}$$

where τ ($= 1/2\pi f_{max}$) is the relaxation time associated with the maximum M'' for a fixed temperature, τ_0 is the relaxation time at very high temperatures, E_a is the activation energy of the relaxation process, k_B is the Boltzmann constant, and T is the temperature. Figure 8 shows the evolution of log τ versus $1/T$ for each one of the different observed relaxations; that is, α and conductivity for the NFRUP and EGMRUP composites. E_a and τ_0 were extracted from the slopes and the intercepts of the plots of log τ versus $1/T$. The mean values of E_a and τ_0 relative to the α relaxation were 136.02 kJ/mol and $10^{-20.96}$ s and 123.2 kJ/mol and 10^{-19} s for the NFRUP and EGMRUP composites, respectively, as mentioned in Table II. However, it can be noted that the incorporation of fibers decreased the apparent activation energy (E_a^{α}) for the two composites in comparison with that for the matrix determined in the previous study; this could be ascribed to the interaction between the fibers and the matrix.[20] This interaction determined the nature of the interfacial adhesion region. The latter was characterized with SEM, as illustrated in the previous section. It also determined the conductivities for the NFRUP composite (96.33 kJ/mol for E_a and $10^{-15.47}$ s for τ_0) and the EGMRUP composite (100 kJ/mol for E_a and $10^{-15.86}$ s for τ_0). These values were in agreement with those reported in other research works.[62]

Table II. Activation Energies E_a and Relaxation Times τ_0 for the NFRUP and EGMRUP Composite Materials.

Composite material	E_a (kJ/mol)	τ_0 (s)
NFRUP		
α Relaxation	136.02	$10^{-20.96}$
Conduction	96.33	$10^{-15.47}$
EGMRUP		
α Relaxation	123.2	10^{-19}
Conduction	100	$10^{-15.86}$

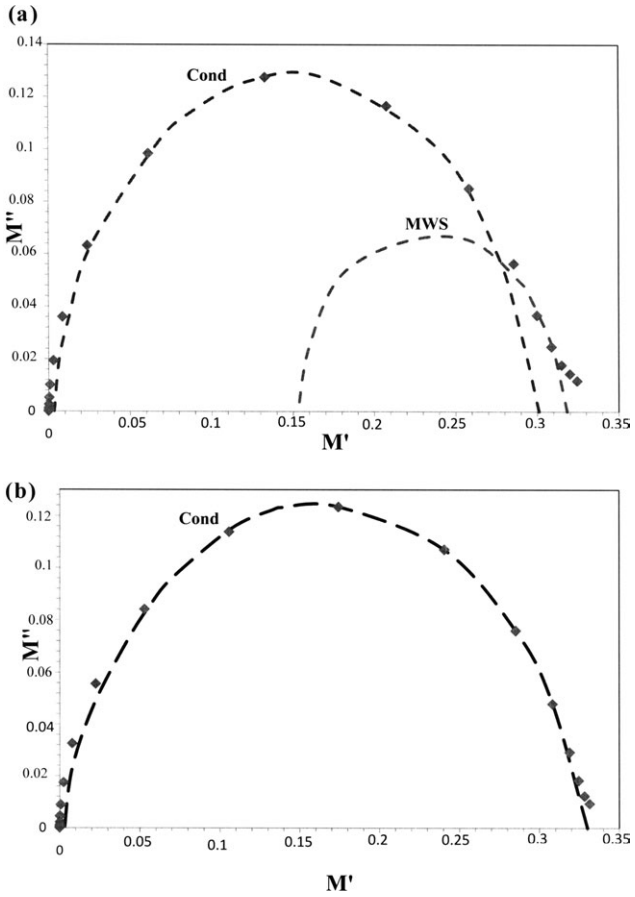

Figure 9. Argand's plots of M^* of the (a) NFRUP and (b) EGMRUP composites at 150°C.

The Argand representation was used to analyze the nature of the relaxation. Cole–Cole plots of the NFRUP and EGMRUP composites at 150°C are depicted in Figure 9(a,b). It has been well established that the response of every relaxation mechanism can be represented very precisely by a model function with four parameters at the most. Among others,[63] this includes the following function:

$$\varepsilon^* = \varepsilon_\infty + \frac{\varepsilon_S - \varepsilon_\infty}{[1 + (i\omega\tau)^\alpha]^\beta} \tag{6}$$

This function was introduced by Havriliak–Negami and is widely used because of its suitability for mathematical processing.[64] In this equation, ε_S and ε_∞ are the dielectric constants on the low- and high-frequency sides of the relaxation, τ is the central relaxation time, ω is the radial frequency, and α and β are fractional shape parameters describing the skewing and broadening of the dielectric function, respectively. Both α and β range between 0 and 1. These coefficients act as the deviation from the Debye equation. In fact, when α and β are equal to 1, this equation reduces to the Debye equation. In the M^* formalism,

Table III. Parameters Evaluated by Data Fitting According to the Havriliak–Negami Equation for the NFRUP and EGMRUP Composites

Composite material	T (°C)	Relaxation	α	β	M_S	M_∞
NFRUP	120	Conduction	0.991	0.947	0.003	0.26
		MWS	0.92	0.892	0.199	0.315
	130	Conduction	0.9915	0.90	0.002	0.295
		MWS	0.901	0.88	0.185	0.3191
	140	Conduction	0.995	0.93	0.002	0.298
		MWS	0.999	0.92	0.21	0.316
	150	Conduction 0.999	0.904	0.0033	0.301	
		MWS	0.99	0.863	0.153	0.3182
EGMRUP						
	120	Conduction	0.9957	0.889	0.0052	0.31
	130	Conduction	0.995	0.83	0.005	0.32
	140	Conduction	0.999	0.819	0.00399	0.3269

the Havriliak–Negami equations [eqs. (7) and (8)] have the following form:[64]

$$M' = M_\infty \frac{[M_s A^\beta + (M_\infty - M_s)\cos\beta\varphi]A^\beta}{M_S^2 A^{2\beta}(M_\infty - M_s)M_s\cos\beta\varphi + (M_\infty - M_s)^2} \quad (7)$$

$$M'' = M_\infty M_s \frac{[(M_\infty - M_s)\sin\beta\varphi]A^\beta}{M_s^2 A^{2\beta}(M_\infty - M_s)M_s\cos\beta\varphi + (M_\infty - M_s)^2} \quad (8)$$

where

$$M_s = \frac{1}{\varepsilon_s} \quad (9)$$

$$M_\infty = \frac{1}{\varepsilon_\infty} \quad (10)$$

$$A = [1 + 2(\omega\tau)^{1-\alpha}\sin\frac{\alpha\pi}{2} + (\omega\tau)^{2(1-\alpha)}]^{1/2} \quad (11)$$

$$\varphi = \text{arctg}[\frac{(\omega\tau)^{2-\alpha}\cos\varepsilon\frac{\alpha\pi}{2}}{1 + (\omega\tau)^{1-\alpha}\sin\frac{\alpha\pi}{2}}] \quad (12)$$

Accordingly, dotted curves were produced by the best fitting experimental points with the Havriliak–Negami equations [eqs. (7) and (8)]. In Figure 9(b), the Cole–Cole diagram corresponded to the conductivity effect for the EGMRUP composite, whereas in Figure 8(a), it is shown that it was impossible to fit the Havriliak–Negami model to all of the experimental points for the NFRUP composites. So, two semicircles were obtained at every examined temperature. The first one for $0 < M' < 0.3$ was related to the conduction effect, and the second one for $0.15 < M' < 0.32$ was linked to the MWS effect. This analysis confirmed the presence of the MWS relaxation, which is overlapped with the dc conductivity effect. The parameters evaluated by the fitting data are listed in Table III. To determine the parameters characteristics of the Havriliak–Negami model (α, β, M_S, and M_∞), the experimental M'_{exp} and M''_{exp} data were smoothed through a numerical simulation in the complex plane. The purpose of such a simulation was to find the theoretical values (M'_{th} and M''_{th}). The values of α, β, M_S, and M_∞ that best smoothed the Havriliak–Negami data were obtained by a successive approach method, in which the following expressions were minimized:

$$\chi^2_{M'} = \sum\nolimits_i (M'_{th} - M'_{exp})^2 \quad (13)$$

$$\chi^2_{M''} = \sum\nolimits_i (M''_{th} - M''_{exp})^2 \quad (14)$$

It has been proven that only one quadruplet value was able to tone with these conditions. Although the values of α and β obtained for the conductive effect were in harmony with a pure Debye type, the values of α and β obtained for interfacial polarization were in accordance with the Havriliak–Negami response.

CONCLUSIONS

A comparative study between natural-fiber–matrix (NFRUP) and E-glass–matrix (EGMRUP) composites for thermal and dielectric properties was undertaken. The UP resin was used as a matrix for both of them. The thermal study (DSC) carried out on these samples showed a variation in T_g as fibers (natural or mineral) were added in the matrix, and this revealed the interaction of the fibers with the matrix. The dielectric response of these composites showed the presence of two common dielectric relaxations, which were attributed to the α relaxation of the polymer and to ionic conduction, which occurred above the glass transition and at low frequencies, respectively. The dielectric analysis revealed that interfacial polarization could not be analyzed by the Argand representation in the EGMRUP composite, as it was absent, whereas in the case of the NFRUP composite, the analysis of the MWS polarization exhibited a consistency of this polarization with the Havriliak–Negami model. The tensile properties of these composites evidenced a slight enhancement in the fiber–matrix adhesion in favor of the NFRUP composite. As a parameter closely related to the static stress transfer at the interface, the Young's modulus showed a slight enhancement in the NFRUP composite compared with that in the EGMRUP composite. Moreover, this comparative experimental study demonstrated that natural fibers enhanced the thermal insulation in the NFRUP composite according to the

dielectric properties, whereas the E-glass fibers strengthened the EGMRUP composite according to the tensile properties.

REFERENCES

1. Cunha, A. M.; Liu, Z. Q.; Feng, Y.; Yi, X. S.; Bernardo, C. A. *J. Mater. Sci.* **2001**, *3*, 4903.
2. Han, Y. H.; Han, S. O.; Cho.D.; Kim, H. I. *Macromol. Res.* **2008**, *16*, 253.
3. Miao, M.; Finn, N. J. *Text. Eng.* **2008**, *54*, 165.
4. Thwe, M. M.; Liao.K. *J. Mater. Sci.* **2003**, *38*, 363.
5. Zah, R.; Hischier, R.; Leao, A. L.; Braun, I. J. *Clean. Prod.* **2007**, *15*, 1032.
6. Eichhorn, S. J.; Baillie, C. A.; Zafeiropoulos, N.; Mwaikambo, L. Y.; Ansell, M. P.; Dufresne, A.; Entwistle, K. M.; Herrera-Franco, P. J.; Escamilla, G. C.; Groom, L.; Hughes, M.; Hill, C.; Rials, T. G.; Wild, P. M. J. *Mater. Sci.* **2001**, *36*, 2107.
7. Gautier, R.; Joly, C.; Coupas, A. C.; Gauthier, H.; Escoubes, M. *Polym. Compos.* **1998**, *19*, 87.
8. Ben Brahim, S.; Ben Cheikh, R. *Compos. Sci. Technol.* **2007**, *67*, 140.
9. Ben Abderrahmane, M.; Ben Cheikh, R. *Surf. Eng. Appl. Electrochem.* **2008**, *44*, 484.
10. Bessadok, A.; Roudesli, S.; Marais, S.; Follain, N.; Lebrun, L. Compos. *A* **2009**, *40*, 184.
11. Maafi, E. M.; Malek, F.; Tighzert, L.; Dony, P. *J. Polym. Environ.* **2010**, *18*, 638.
12. Ghallabi, Z.; Rekik, H.; Boufi, S.; Arous, M.; Kallel, A. *J. Non-Cryst. Solids.* **2010**, *356*, 684.
13. Arous, M.; Ben Amor, I.; Boufi, S.; Kallel, A. *J. Appl. Polym. Sci.* **2007**, *106*, 3631.
14. Ben Brahim, S.; Ben Cheikh, R. *Compos. Sci. Technol.* **2007**, *67*, 140.
15. Manfredi, L. B.; Rodriguez, E. S.; Wladyka-Przybylak, M.; Vazquez, A. *Polym. Degrad. Stab.* **2006**, *91*, 255.
16. Luo, S.; Netravali, A. *Polym. Compos.* **1999**, *20*, 367.
17. Racz, I.; Hargitai, H. *Int. J. Polym. Mater.* **2000**, *47*, 667.
18. Mishra, S.; Mohanty, A. K.; Drzal, L. T.; Misra, M.; Parija, S.; Nayak, S. K.; Tripathy, S. S. *Compos. Sci. Technol.* **2003**, *63*, 1377.
19. Ben Amor, I.; Rekik, H.; Kaddami, H.; Raihane, M.; Arous, M.; Kallel, A. *J. Compos. Mater.* **2010**, *44*, 1553.
20. Triki, A.; Guicha, M.; Ben Hassen, M.; Arous, M.; Fakhfakh, Z. *J. Mater. Sci.* **2011**, *46*, 3698.
21. Güneri, A.Handbook of Composite Fabrication;Kaynak, C., Akgul, T., Eds.; Polestar Scientifica: Exeter, United Kingdom, **2001**; Chapter 3, p 57.
22. Guicha, M.; Hlimi, M. T.; Ben Hassan, M.; Sakli, F. (to INNORPI.). Pat. Appl. TN 2009/0200 (2000; in accordance with law number 2000–84).
23. Belaabed, B.; Wojkiewicz, J. L.; Lamouri, S.; El Kamchi, N.; Redon, N. *Polym. Adv. Technol.* **2011**, *23*, 1194.
24. Kaddami, H.; Dufresne, A.; Khelifi, B.; Bendahou, A.; Taourirte, M.; Raihane, M.; Issartel, N.; Sautereau, H.; Gérard, J. F.; Sami, N. Compos. *A* **2006**, *37*, 1413.
25. Azimi, H. R.; Pearson, R. A.; Hertzberg, R. W. *J. Appl. Polym. Sci.* **1995**, *58*, 449.
26. Urbaczewski-Espuche, E.; Gerard, J. F.; Pascault, J. P.; Sautereau, H. *J. Appl. Polym. Sci.* **1993**, *47*, 991.
27. Sautereau, H.; Maazouz, A.; Gerard, J. F.; Trotignon, J. P. *J. Mater. Sci.* **1995**, *30*, 1715.
28. Ash, B. J.; Schadler, L. S.; Siegel, R. W.; Apple, T.; Benicewicz, B. C.; Roger, D. F.; Wiegand, C. J. Polym. *Compos* **2002**, *23*, 1014.
29. Cousin, P.; Smith.P. *J. Polym. Sci. Part B: Polym. Phys.* **1994**, *32*, 459.
30. Fréchette, M. F.; Trudeau, M.; Alamdari, H. D.; Boily, S. *IEEE Conf. Electr. Insul. Dielectr. Phenom.* **2001**, 92.
31. Binder, K.; Baschnagel, J.; Bennemann, C.; Paul, W. *J. Phys. Condens. Matter* **1999**, *11*, A47.
32. Doruker, P.; Mattice, L. W. *Macromolecules* **1999**, *32*, 194.
33. Mansfield, K. F.; Theodorou, D. N. *Macromolecules* **1991**, *24*, 6283.
34. Baschnagel, J.; Binder, K. *Macromolecules* **1995**, *28*, 6808.
35. Pham, J. Q.; Mitchell, C. A.; Bahr, J. L.; Tour, J. M.; Krishanamoorti, R.; Green, P. F. *J. Polym. Sci. Part B: Polym. Phys.* **2003**, *41*, 3339.
36. Schulte, K.; Gojny, F. H.; Fiedler, B.; Sandler, J. K. W.; Bauhoer, W. In Polymer Composites from Nano- to Macro-Scale; Friedrich, K., Fakirov, S., Zhang, Z., Eds.; Springer:-New York, **2005**; Chapter 1, p 3.
37. Zhang, M. Q.; Rong, M. Z.; Friedrich, K. In Polymer Composites from Nano- to Macro-Scale; Friedrich, K., Fakirov, S., Zhang, Z., Eds.; Springer: New York, **2005**; Chapter 2, p 25.
38. Sawpan, M. A.; Pickering, K. L.; Fernyhough, A. *Comp. A : Appl. Sci & Manuf* **2011**, *42*, 1189.
39. Vilay, V.; Mariatti, M.; Mat Taib, R.; Todo, M. *Compos. Sci. Technol.* **2008**, *68*, 631.
40. Kim, J. K.; Mai, Y. W. *Compos. Sci. Technol.* **1991**, *41*, 333.
41. Sham, M. L.; Kim, J. K.; Wu, J. S. *Polym. Polym. Compos.* **1997**, *5*, 165.
42. Yim, A.; Chahal, R. S.; St.-Pierre, L. E. *J. Colloid Interface Sci.* **1973**, *43*, 583.
43. Lisaka, K.; Shibayma, K. *J. Appl. Polym. Sci.* **1978**, *22*, 3135.
44. Brahim, S. B.; Cheikh, R. B. *Compos. Sci. Technol.* **2007**, *67*, 140.
45. Arbelaiz, A.; Fernandez, B.; Cantero, G.; Llano-Ponte, R.; Valea, A.; Mondragon, I. Compos. *A* **2005**, *36*, 1637.
46. Rozman, H. D.; Saad, M. J.; Mohd Ishak, A. *J. Appl. Polym. Sci.* **2003**, *87*, 827.
47. Van den Over, M. J. A.; Bos, H. L.; Van Kemenade, M. J. J. M. *Appl. Compos. Mater.* **2000**, *7*, 387.
48. Oksman, K. *Appl. Compos. Mater.* **2000**, *7*, 403.
49. Thwe, M. M.; Liao, K. *Compos. Sci. Technol.* **2003**, *63*, 375.
50. Li, Y.; Mai, Y.; Ye, L. *Compos. Sci. Technol.* **2000**, *60*, 2037.
51. Kumar, S.; Choudhary, V.; Kumar, R. *J. Therm. Anal. Calorim.* **2010**, *102*, 751.

52. Tsangaris, G. M.; Psarras, G. C.; Kontopoulos, A. J. *J. Non--Cryst. Solids* **1991**, *131–133*, 1164.

53. Patra, A.; Bisoyi, D. K. *J. Mater. Sci.* **2010**, *45*, 5742.

54. Hammami, H.; Arous, M.; Lagache, M.; Kallel, A. Compos. *A* **2006**, *37*, 1.

55. Okrassa, L.; Boiteux, G.; Ulanski, J.; Seytre, G. *Polymer* **2001**, *42*, 3817.

56. Perrier, G. *Recent Res. Dev. Polym. Sci.* **1995**, *3*, 175.

57. Uhlmann, D. R.; Kreidl, N. J. Glass Science and Technology. Volume 4A. Structure, Microstructure and Properties; Kapitel 2–4; Academic:San Diego, **1990**.

58. Howard, W.; Starkweather, J. R.; Avakian, P. *J. Polym. Sci. Part B: Polym. Phys.* **1992**, *30*, 637.

59. Tsangaris, G. M.; Psarras, G. C.; Kouloubi, N. *J. Mater. Sci.* **1998**, *33*, 2027.

60. Sambasiva Rao, K.; Madhava Prasad, D.; Murali Krishna, P.; Swarna Latha, T.; Hyung Lee, J. *Optoelectron. Adv. Mater. Rapid Commun.* **2007**, *1*, 510.

61. Nanda, M.; Tripathy, D. K. *Express Polym. Lett.* **2008**, *2*, 855.

62. Ben Amor, I.; Rekik, H.; Kaddami, H.; Raihane, M.; Arous, M.; Kallel, A. *J. Electrostat.* **2009**, *67*, 717.

63. Hill, R. M. Phys. *Status Solidi B* **1981**, *103*, 319.

64. Havriliak, S.; Negami, S. *J. Polym. Sci. Part C: Polym. Lett.* **1966**, *14*, 99.